Dalton Transactions

Accepted Manuscript

ROYAL SOCIETY OF CHEMISTRY

www.rsc.org/dalton

Journal Name

Paper

Cascade approach to hetero-pentanuclear manganese-oxide clusters in polyoxometalates and their single-molecule magnet properties†

Received 00th January 20xx,
Accepted 00th January 20xx

DOI: 10.1039/x0xx00000x

www.rsc.org/

Kosuke Suzuki, Rinta Sato, Takuo Minato, Masahiro Shinoe, Kazuya Yamaguchi and Noritaka Mizuno*

Structurally well-defined hetero-pentanuclear manganese-oxide clusters {MMn_4} were successfully synthesized in $TBA_7H_n[MMn_4(OH)_2(A\text{-}\alpha\text{-}SiW_9O_{34})_2]\cdot 2H_2O\cdot C_2H_4Cl_2$ (**II$_{MMn4}$**, M = Fe(III), Co(II), Ni(II), Cu(II), Ga(III)) by sequential introduction of metal cations into the trivacant lacunary polyoxometalates (POMs). The pentanuclear manganese-oxide cluster {Mn_5} showed small spin ground state and low energy barrier for magnetization relaxation. In contrast, the magnetic interactions in the hetero-pentanuclear clusters could be controlled by the arrangements of metals, and the clusters showed the large magnetic anisotropy and the single-molecule magnet behavior. In particular, the cluster {$FeMn_4$} in **II$_{FeMn4}$** (S = 11/2) showed the slowest relaxation and the highest energy barrier among the previously reported transition metal-containing POMs.

Introduction

Polyoxometalates (POMs) are a remarkable class of structurally well-defined discrete metal-oxide clusters with broad structural and compositional versatility, and they are attractive materials in various fields of science.[1] In particular, lacunary POMs with coordination sites for additional metal cations are useful multidentate inorganic ligands for constructing transition metal-oxide clusters with various catalytic, photocatalytic, magnetic, and electrochemical properties.[2] In addition, they are thermally and oxidatively stable in comparison with commonly utilized organic ligands, and the bulky diamagnetic POM ligands can effectively isolate the metal cores to prevent unnecessary intermolecular magnetic interaction and polymerization. Therefore, they can provide ideal models to study the intrinsic nature of metal-oxide clusters.

Recently, manganese-based metal-oxide clusters have received considerable interests because of their unique properties, such as oxygen evolution catalysis in photosystem II (PS II)[3] and single-molecule magnet (SMM) properties with large magnetic anisotropy.[4] As observed for the heteronuclear cores in PS II {Mn_4Ca} and SMMs, the introduction of the second metal atoms into the manganese-oxide clusters is the important factors to control their redox, catalytic, and magnetic properties.[4e-g,5] Therefore, the development of efficient synthetic methods for heteronuclear clusters based on the precise design of the structures (that is, arrangements of metals, types of bridging ligands, and interactions) is indispensable.

We have developed various multinuclear metal-containing POMs with unique catalytic, photocatalytic, and magnetic properties by the reaction of metal cations with lacunary POMs in organic media.[6] In particular, we have recently reported the SMMs by controlling the coordination geometries of metal cations in POMs.[6c,d] We envisaged that efficient SMMs could be constructed by precise design of arrangements and interactions of manganese cations in multinuclear clusters, and herein successfully synthesized hetero-multinuclear manganese-oxide cores in POMs **II$_{MMn4}$** ($TBA_7H_n[MMn_4(OH)_2(A\text{-}\alpha\text{-}SiW_9O_{34})_2]\cdot 2H_2O\cdot C_2H_4Cl_2$ (M = Fe(III), Co(II), Ni(II), Cu(II), Ga(III)) by sequential introduction of metal cations into the lacunary POMs (Fig. 1).[7] The clusters showed the large magnetic anisotropy and the unique SMM behavior.

Results and discussion

Synthesis and magnetic property of a pentanuclear manganese-oxide cluster

Initially, a pentanuclear manganese-oxide cluster was synthesized by the reaction of a trivacant lacunary POM $TBA_4H_6[A\text{-}\alpha\text{-}SiW_9O_{34}]\cdot 2H_2O$ (**SiW9**)[8] with 2.5 equivalents of $Mn(acac)_3$ (acac = acetylacetonato) in acetone. The X-ray crystallographic analysis showed the formation of the pentanuclear {$Mn(III)_5O_{18}(OH)_2$} cluster in **Mn5** ($TBA_7[Mn_5(OH)_2(A\text{-}\alpha\text{-}SiW_9O_{34})_2]\cdot 2H_2O\cdot C_2H_4Cl_2$, Figs. 1, S1, Tables 1, S1, S2, ESI†). Notably, the axial ligands of the five Mn(III) aligned to the similar direction in the cluster, suggesting the presence of large magnetic anisotropy desirable for SMMs. The alternating current (ac) magnetic susceptibility measurement of **Mn5** showed the temperature- and

Department of Applied Chemistry, School of Engineering, The University of Tokyo, 7-3-1 Hongo, Bunkyo-ku, Tokyo 113-8656, Japan. E-mail: tmizuno@mail.ecc.u-tokyo.ac.jp; Fax: (+)81-3-5841-7220

† Electronic Supplementary Information (ESI) available: Experimental details including syntheses, crystallographic data, IR and CSI-MS spectra, and magnetic data. For ESI and crystallographic data in CIF or other electronic format see DOI: 10.1039/x0xx00000x

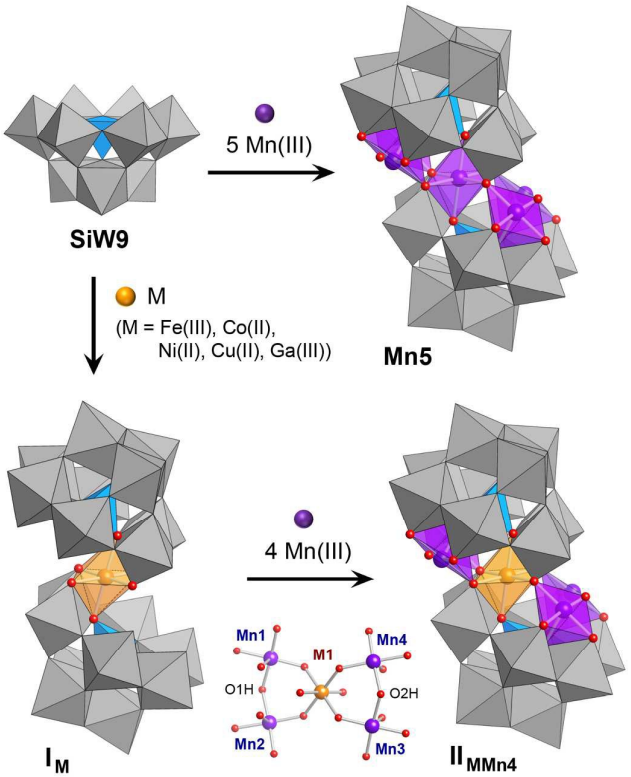

Fig. 1 Schematic representation of the formation of pentanuclear manganese-containing POM **Mn5** and hetero-pentanuclear transition metal-containing POMs $\mathbf{II}_{MMn4}$ (M = Fe(III), Co(II), Ni(II), Cu(II), Ga(III)) from $TBA_4H_6[A\text{-}\alpha\text{-}SiW_9O_{34}]$ via mononuclear metal-containing POMs $\mathbf{I}_M$. Inset: top view of the $\{MMn_4\}$ core in $\mathbf{II}_{MMn4}$. Orange, purple, and red spheres represent M, manganese, and oxygen atoms, respectively, and gray and light blue polyhedra represent tungsten and silicon, respectively.

frequency-dependent in-phase (χ') and out-of-phase signals (χ'') characteristic for SMMs under the zero external direct current (dc) field (Fig. S2, ESI†). Although **Mn5** possessed five Mn(III) (S = 2), the dc magnetic susceptibility and magnetization data indicated that the spin ground state was S = 2,[9] and the thermal energy barrier for magnetization relaxation (U_{eff}) was 19.5 K (13.6 cm^{-1}, Table S4, ESI†) according to the Arrhenius plots ($\ln\tau$ ($\tau = \tau_0\exp(U_{eff}/k_BT)$) *vs* T^{-1}, Fig. S3, ESI†).[10] The best fit of the temperature-dependence of magnetic susceptibility with the Heisenberg–Dirac–Van Vleck Hamiltonian showed that the exchange interactions of J_1 (−4.10 cm^{-1}) and J_2 (−3.60 cm^{-1}) are similar negative values (Fig. 2),[11] which likely resulted in the small spin ground state. These results indicated that, based on the large anisotropy in the pentanuclear cluster, efficient SMMs would be developed by controlling the magnetic interaction and spin ground state via introduction of the second paramagnetic transition metals, such as Fe(III), Co(II), Ni(II), and Cu(II).

Synthesis of hetero-pentanuclear manganese-oxide clusters in POMs

Based on the above-mentioned idea, synthesis of hetero-pentanuclear clusters for SMMs was initially attempted by

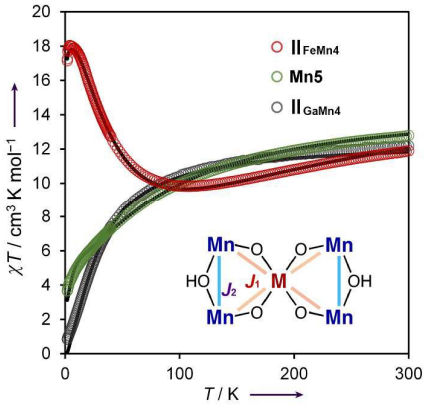

Fig. 2 Temperature dependence of χT for **Mn5**, $\mathbf{II}_{FeMn4}$, and $\mathbf{II}_{GaMn4}$ under the applied field of 0.1 T. Solid lines represent the best fits adopting the Heisenberg–Dirac–Van Vleck Hamiltonian.

mixing two types of metal cations with **SiW9** simultaneously. For clear discussion of the mass spectra, Ga(III) with markedly different atomic weights from Mn(III) was used for the test reaction. Disappointingly, by the simple mixing of $Ga(acac)_3$, $Mn(acac)_3$, and **SiW9** (1:4:2 molar ratio) in 1,2-dichloroethane, the cold-spray ionization (CSI) mass spectrum showed the sets of signals centered at *m/z* 6421, 6510, 6597, 6652, and 6701 assignable to $[TBA_8H_6Mn(SiW_9O_{33})_2]^+$, $[TBA_8H_7Mn_2(SiW_9O_{34})_2]^+$, $[TBA_8H_8Mn_3O_2(SiW_9O_{34})_2]^+$, $[TBA_8H_5Mn_4O_2(SiW_9O_{34})_2]^+$, and $[TBA_8H_2Mn_5O_2(SiW_9O_{34})_2]^+$, respectively (Fig. S4, ESI†). Although the desired hetero-pentanuclear structures could not be synthesized by the direct one-step synthesis, we obtained an important finding that the metal cations are sequentially introduced into the lacuna of $[A\text{-}\alpha\text{-}SiW_9O_{34}]^{10-}$ units.

To date, several synthetic methods for heteronuclear metal-oxide clusters in POMs have been reported in aqueous media (Fig. S5, ESI†): (a) Heteronuclear metal-oxide clusters have been synthesized by the reaction of two types of metal cations with starting reagents (such as Na_2WO_4, Na_2HAsO_4),[12] or (b) by the reaction of two types of metal cations with lacunary POMs in one step.[13] Because these two methods are often accompanied by isomerization of POMs, it is difficult to predict the structures of the metal-oxide clusters in the products. (c) The synthetic method by exchange of the substituted metals or temporally placed counter cations in POMs with other metal cations has also been reported.[14] This method is sometimes troubling because of the non-quantitative exchange of metal cations and/or the limitation of applicability. Therefore, the truly effective methods for synthesis of structurally well-defined heteronuclear clusters should be developed.

Herein, we focused on the sequential introduction of the metal cations into the lacuna of POMs in organic media.[6f] Very recently, we have reported the synthesis of mononuclear transition metal-containing POMs ($\mathbf{I}_M$, M = Fe(III), Co(II), Mn(III), Fig 1) by the reactions of **SiW9** with $M(acac)_n$.[15] Although $\mathbf{I}_M$ showed the SMM behavior with mononuclear

Table S1. Crystallographic data for **Mn5**, $\mathbf{II}_{\mathbf{FeMn4}}$, $\mathbf{II}_{\mathbf{CoMn4}}$, $\mathbf{II}_{\mathbf{NiMn4}}$, $\mathbf{II}_{\mathbf{CuMn4}}$, and $\mathbf{II}_{\mathbf{GaMn4}}$

	Mn5	$\mathbf{II}_{\mathbf{FeMn4}}$	$\mathbf{II}_{\mathbf{CoMn4}}$	$\mathbf{II}_{\mathbf{NiMn4}}$	$\mathbf{II}_{\mathbf{CuMn4}}$	$\mathbf{II}_{\mathbf{GaMn4}}$
formula	$C_{118}Cl_6Mn_5N_7O_{70}Si_2W_{18}$	$C_{120}Cl_8FeMn_4N_7O_{70}Si_2W_{18}$	$C_{120}Cl_8CoMn_4N_7O_{70}Si_2W_{18}$	$C_{120}Cl_8Mn_4N_7NiO_{70}Si_2W_{18}$	$C_{120}Cl_8CuMn_4N_7O_{70}Si_2W_{18}$	$C_{116}GaMn_4N_{11}O_{78}Si_2W_{18}$
Fw (g mol^{-1})	6488.13	6583.96	6587.04	6586.82	6591.65	6450.23
cryst system	triclinic	triclinic	triclinic	triclinic	triclinic	monoclinic
space group	*P*-1 (#2)	*P*-1 (#2)	*P*-1 (#2)	*P*-1 (#2)	*P*-1 (#2)	$P2_1/c$ (#14)
□ (Å)	14.3048(2)	14.29940(10)	14.34670(10)	14.34280(10)	14.36010(10)	28.57090(10)
□ (Å)	20.0807(2)	20.0839(2)	20.20680(10)	20.17370(10)	20.2319(2)	22.31140(10)
c□(Å)	34.0794(4)	34.1530(5)	34.2447(3)	34.2468(3)	34.2700(3)	29.6879(2)
α (deg)	102.5990(5)	102.4537(9)	103.6296(5)	103.4637(4)	103.5415(6)	90
β (deg)	96.6992(5)	96.6522(9)	97.2188(4)	97.1819(4)	97.3195(4)	104.9980(10)
γ (deg)	93.5217(6)	93.5185(4)	92.9884(6)	93.1231(5)	92.9779(4)	90
V (Å^3)	9450.2(2)	9475.28(18)	9537.06(12)	9525.33(12)	9566.28(15)	18280.07(18)
Z	2	2	2	2	2	4
temp (K)	123(2)	123(2)	123(2)	123(2)	113(2)	123(2)
ρ_{calcd} (g cm^{-3})	2.280	2.308	2.294	2.297	2.288	2.344
GOF	1.021	1.026	1.045	1.031	1.101	1.060
R_1 [$I>2\sigma(I)$]	0.0787 (for 30531 data)	0.0561 (for 39174 data)	0.0496 (for 43894 data)	0.0507 (for 44172 data)	0.0585 (for 44204 data)	0.0451 (for 41698 data)
wR_2	0.1790 (for all 49331 data)	0.1455 (for all 51766 data)	0.1272 (for all 52081 data)	0.1378 (for all 52105 data)	0.2015 (for all 52203 data)	0.1231 (for all 50339 data)

paramagnetic metals (single-ion magnet, SIM), they required the external dc field to achieve the SMM behavior because of the considerable effects of magnetic relaxations by quantum tunneling and/or easy-plane type magnetic anisotropy. Notably, these POMs possessed unique coordination sites for the additional metal cations, which are stabilized by multiple hydrogen bonding networks. Because $\mathbf{I}_\mathbf{M}$ possessed the partial structures of **Mn5** except for peripheral four Mn(III) cations, we envisaged that a series of $\mathbf{I}_\mathbf{M}$ can be utilized as "structural motifs" for the synthesis of heterometal-containing manganese-oxide clusters {MMn_4}.

Fortunately, a novel hetero-pentanuclear {$FeMn_4$}-containing POM $\mathbf{II}_{\mathbf{FeMn4}}$ was successfully synthesized by the reaction of $\mathbf{I}_{\mathbf{Fe}}$ with four equivalents of $Mn(acac)_3$ in 1,2-dichloroethane (see ESI† for detail). By addition of diethyl ether to the reaction solution, dark green single crystals suitable for X-ray crystallographic analysis were successfully obtained. The CSI-mass spectra of both the reaction solution and the crystals dissolved in 1,2-dichloroethane showed the sets of signals centered at *m/z* 3473 and 6703 assignable to $[TBA_9H_2FeMn_4O_2(SiW_9O_{34})_2]^{2+}$ and $[TBA_8H_2FeMn_4O_2(SiW_9O_{34})_2]^{+}$, respectively, indicating the quantitative introduction of four Mn(III) cations into the lacuna of $\mathbf{I}_{\mathbf{Fe}}$ (Fig. 3a). The anion structure of $\mathbf{II}_{\mathbf{FeMn4}}$ consisted of the pentanuclear metal core and two sandwiching [A-α-SiW_9O_{34}]$^{10-}$ units and was essentially isostructural with that of **Mn5** (Figs. 1, S7, Table 1, S1, S2, ESI†). Four Mn(III) cations were arranged around the central Fe(III), forming the unique bow tie type hetero-pentanuclear structure. The bond valence sum (BVS) values of the bridging oxygen atoms (O1H and O2H) between Mn(III) cations were 1.16 and 1.17, indicating that these oxygen atoms were protonated (hydroxo ligands, Table S2, ESI†).

In the similar way, the pentanuclear structures with different paramagnetic metals ($\mathbf{II}_{\mathbf{MMn4}}$; M = Co(II), Ni(II), Cu(II)) were synthesized by the reaction of the corresponding mononuclear transition metal-containing lacunary structures $\mathbf{I}_\mathbf{M}$ (M = Co(II), Ni(II), Cu(II))[16] with $Mn(acac)_3$ (four equivalents with respect to $\mathbf{I}_\mathbf{M}$, Fig. 1). POM $\mathbf{II}_{\mathbf{GaMn4}}$ with the central diamagnetic Ga(III) was also synthesized for the comparison of magnetic data (Fig. 3b). It should be noted that $\mathbf{II}_{\mathbf{MMn4}}$ as well as $\mathbf{II}_{\mathbf{GaMn4}}$ could not be synthesized by the direct one-step reaction of M (M ≠ Mn(III)), Mn(III), and **SiW9** as mentioned above. These pentanuclear structures were intrinsically isostructural with $\mathbf{II}_{\mathbf{FeMn4}}$ (Figs. S8–S11, Table 1, S1, S2, ESI†). The X-ray crystallography, CSI-mass spectra (Figs. 3, S6, ESI†), and elemental and thermogravimetric analyses showed that the molecular formulas of $\mathbf{II}_{\mathbf{MMn4}}$ were $TBA_7H_n[MMn_4(OH)_2(A\text{-}\alpha\text{-}SiW_9O_{34})_2]\cdot 2H_2O\cdot C_2H_4Cl_2$ (for M = Fe(III), Ga(III), n = 0; for M = Co(II), Ni(II), Cu(II), n = 1). Although trivacant lacunary Keggin-type POMs have been utilized as the multidentate ligands for the syntheses of various multinuclear cores with unique properties, there has been no report on this type of pentanuclear structure.

Single-molecule magnetic properties of hetero-pentanuclear manganese-oxide clusters in POMs

To investigate their magnetic interactions and SMM properties, the magnetic susceptibility measurements were carried out for the polycrystalline samples. The dc magnetic susceptibilities

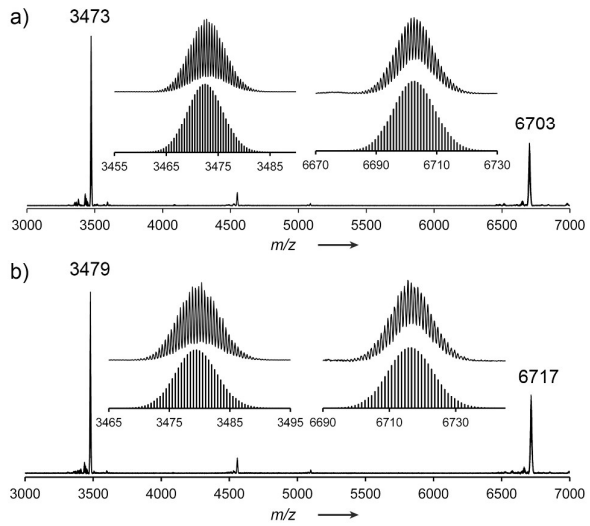

Fig. 3 Positive-ion CSI-mass spectra of (a) $\mathbf{II}_{\mathbf{FeMn4}}$ and (b) $\mathbf{II}_{\mathbf{GaMn4}}$ in 1,2-dichloroethane. The sets of signals centered at *m/z* 3473, 6703, 3479, and 6717 were assignable to $[TBA_9H_2FeMn_4O_2(SiW_9O_{34})_2]^{2+}$, $[TBA_8H_2FeMn_4O_2(SiW_9O_{34})_2]^{+}$, $[TBA_9H_2GaMn_4O_2(SiW_9O_{34})_2]^{2+}$, and $[TBA_8H_2GaMn_4O_2(SiW_9O_{34})_2]^{+}$, respectively.

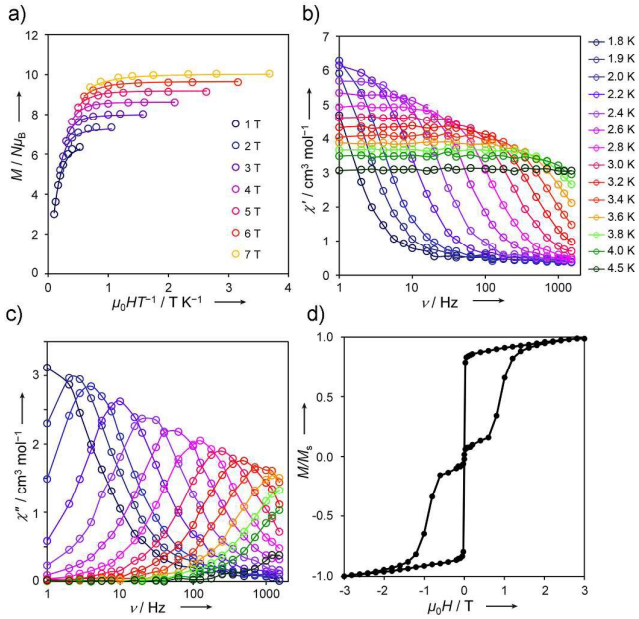

Fig. 4 Magnetic data for $\mathbf{II}_{\mathbf{FeMn4}}$. (a) Low temperature magnetization data (solid lines represent the best fits adopting the Hamiltonian given in eqn (1)). Frequency dependence of the alternating current magnetic susceptibility ((b) χ' and (c) χ'') under the zero external dc field. (d) Magnetization versus magnetic field data of polycrystalline sample of $\mathbf{II}_{\mathbf{FeMn4}}$ at 0.5 K (sweeping late, ca 0.08 T min^{-1}).

under the external field of 0.1 T showed that the χT values at 300 K for $\mathbf{II}_{\mathbf{FeMn4}}$, $\mathbf{II}_{\mathbf{CoMn4}}$, $\mathbf{II}_{\mathbf{NiMn4}}$, and $\mathbf{II}_{\mathbf{CuMn4}}$ were 11.90,11.79, 11.53, and 12.20 cm^3 K mol^{-1}, respectively (Figs. 2, S12, ESI†). These values were smaller than sums of the spin-only values for four high spin Mn(III) (3.00 cm^3 K mol^{-1}; $S = 2$, $g = 2.00$) and the central paramagnetic metals, which is likely due to the antiferromagnetic interactions and/or magnetic anisotropy. The χT value at 300 K for $\mathbf{II}_{\mathbf{GaMn4}}$ was 12.18 cm^3 K mol^{-1} close to the spin-only value for four high-spin Mn(III). The χT values for $\mathbf{II}_{\mathbf{MMn4}}$ gradually decreased with decreasing temperature and then increased below ca. 90 ($\mathbf{II}_{\mathbf{FeMn4}}$, $\mathbf{II}_{\mathbf{CuMn4}}$) and 60 K ($\mathbf{II}_{\mathbf{CoMn4}}$, $\mathbf{II}_{\mathbf{NiMn4}}$), and reached to the values of 18.0 (at 3.9 K, $\mathbf{II}_{\mathbf{FeMn4}}$), 13.9 (2.9 K, $\mathbf{II}_{\mathbf{CoMn4}}$), 17.3 (2.9 K, $\mathbf{II}_{\mathbf{NiMn4}}$), and 21.9 cm^3 K mol^{-1} (4.4 K, $\mathbf{II}_{\mathbf{CuMn4}}$), respectively (Figs. 2, S12, ESI†). According to the reported procedures for analysis of magnetization data of polynuclear metal-oxide clusters, the magnetization vs HT^{-1} data were fitted by the Hamiltonian given in eqn (1) (the parameters D and E represent axial and transverse anisotropy, respectively) (Figs. 4a, S13, ESI†):[17a,b]

$$H = D(S_z^2 - S(S+1)/3) + E(S_x^2 - S_y^2) + \mu_B g\mathbf{SH} \quad (1)$$

The best fit parameters were as follows: $D = -0.734$ cm^{-1}, $|E| = 1.1\times10^{-5}$ cm^{-1}, and $g = 2.03$ ($\mathbf{II}_{\mathbf{FeMn4}}$, $S = 11/2$); $D = -2.08$ cm^{-1}, $|E| = 2.9\times10^{-5}$ cm^{-1}, and $g = 2.41$ ($\mathbf{II}_{\mathbf{CoMn4}}$, $S = 11/2$); $D = -0.205$ cm^{-1}, $|E| = 4.9\times10^{-4}$ cm^{-1}, and $g = 2.15$ ($\mathbf{II}_{\mathbf{NiMn4}}$, $S = 5$); $D = -0.631$ cm^{-1}, $|E| = 1.2\times10^{-4}$ cm^{-1}, and $g = 2.01$ ($\mathbf{II}_{\mathbf{CuMn4}}$, $S = 6$). These data indicated the corresponding spin ground states of 11/2 ($\mathbf{II}_{\mathbf{FeMn4}}$), 11/2 ($\mathbf{II}_{\mathbf{CoMn4}}$), 5 ($\mathbf{II}_{\mathbf{NiMn4}}$), and 6 ($\mathbf{II}_{\mathbf{CuMn4}}$), showing the much larger spin ground states than that of **Mn5** ($S = 2$), as we expected. In addition, the pentanuclear clusters possessed large negative uniaxial anisotropies ($D < 0$, $|E/D| \sim 10^{-5}$). Therefore, the pentanuclear clusters possessed both the large spin ground states and uniaxial anisotropies suitable for SMMs. In contrast, The χT value for $\mathbf{II}_{\mathbf{GaMn4}}$ with the central diamagnetic Ga(III) was 0.84 cm^3 K mol^{-1} at 1.9 K, indicating the spin ground state of ~0. The magnetic interactions were analyzed by fitting the temperature dependence of magnetic susceptibilities (Figs. 2, S12, ESI†).[11] The best fitting parameters are as follows (J_1 and J_2 represent exchange interactions of M–Mn and Mn–Mn, respectively): $J_1 = -7.78$ and $J_2 = -1.17$ cm^{-1} ($\mathbf{II}_{\mathbf{FeMn4}}$), $J_1 = -9.61$ and $J_2 = -3.83$ cm^{-1} ($\mathbf{II}_{\mathbf{CoMn4}}$), $J_1 = -8.40$ and $J_2 = -2.41$ cm^{-1} ($\mathbf{II}_{\mathbf{NiMn4}}$), $J_1 = -10.06$ and $J_2 = -1.30$ cm^{-1} ($\mathbf{II}_{\mathbf{CuMn4}}$), and $J_2 = -2.98$ cm^{-1} ($\mathbf{II}_{\mathbf{GaMn4}}$). These results indicated that the relatively large ground spin states were successfully achieved based on the coexistence of multiple antiferromagnetic interactions in the hetero-pentanuclear clusters. Especially, the spin ground state of $\mathbf{II}_{\mathbf{FeMn4}}$ ($S = 11/2$) was due to the antiferromagnetic interactions between four periphery Mn(III) cations and central Fe(III) cation (11/2 = 4×2 – 5/2). This spin ground state was successfully achieved based on the much larger $|J_1|$ value than $|J_2|$ value. In contrast, $|J_1|$ and $|J_2|$ values of other $\mathbf{II}_{\mathbf{MMn4}}$ were relatively close to each other. As the results, the energy levels of the spin ground states for $\mathbf{II}_{\mathbf{MMn4}}$ were not sufficiently separated from those of other spin states, which likely resulted in the smaller spin ground states than the theoretical values.

The ac magnetic susceptibility measurements for $\mathbf{II}_{\mathbf{MMn4}}$ (M = Fe(III), Co(II), Ni(II), Cu(II)) showed the considerable temperature- and frequency-dependent χ' and χ'' even under the

zero external dc field, indicating the slow relaxation of magnetization characteristic for SMMs (Figs. 4b,c, S14–S17, ESI†).[18] These results were in sharp contrast with the results that the mononuclear structures $\mathbf{I_{Mn}}$, $\mathbf{I_{Fe}}$, and $\mathbf{I_{Co}}$ required the external dc field for the slow magnetic relaxation.[14] In contrast, $\mathbf{II_{GaMn4}}$ with the central diamagnetic Ga(III) showed no slow magnetic relaxation (Fig. S18, ESI†). The Cole-Cole plots for $\mathbf{II_{MMn4}}$ in the form of χ'' vs χ' were fitted using the generalized Debye model,[18] and the small α values of 0.05–0.28 showed the small distribution of relaxation process (Fig. S19, Tables S4–S8, ESI†). According to the Arrhenius plots, the energy barrier for magnetization relaxation (U_{eff}) increased by introduction of central heterometals into the pentanuclear clusters $\{MMn_4\}$ (Fig. S3, Table S3, ESI†): U_{eff} = 31.4 K (22.0 cm^{-1}, $\mathbf{II_{FeMn4}}$), 22.3 K (15.2 cm^{-1}, $\mathbf{II_{CoMn4}}$), 19.4 K (13.5 cm^{-1}, $\mathbf{II_{NiMn4}}$), 23.1 K (16.0 cm^{-1}, $\mathbf{II_{CuMn4}}$). In particular, $\mathbf{II_{FeMn4}}$ showed the slowest relaxation and the highest energy barrier among the previously reported transition metal-containing POMs.[17] Due to the slow relaxation of $\mathbf{II_{FeMn4}}$, the prominent butterfly-shaped hysteresis was observed in the M vs H data at 0.5 K (Fig. 4d).

Conclusions

In conclusion, structurally well-defined hetero-multinuclear transition metal cores in POMs were successfully synthesized by sequential introduction of metal cations. By the reaction of trivacant lacunary POMs with pillared metal cations, followed by the reaction with additional metal cations (Mn(III)) in an organic solvent, hetero-pentanuclear $\{MMn_4\}$-containing POMs $\mathbf{II_{MMn4}}$ ($TBA_7H_n[MMn_4(OH)_2(A\text{-}\alpha\text{-}SiW_9O_{34})_2]\cdot 2H_2O\cdot C_2H_4Cl_2$ (M = Fe(III), Co(II), Ni(II), Cu(II), Ga(III)) could selectively be obtained. The magnetic interactions in hetero-pentanuclear clusters $\{MMn_4\}$ could be controlled by the arrangements of metals, and $\mathbf{II_{MMn4}}$ with central paramagnetic metals showed the large magnetic anisotropy and the SMM behavior.

Experimental

Materials

$TBA_4H_6[A\text{-}\alpha\text{-}SiW_9O_{34}]\cdot 2H_2O$ (**SiW9**),[8] $TBA_7H_{10}[Fe(A\text{-}\alpha\text{-}SiW_9O_{34})_2]\cdot 2H_2O\cdot C_2H_4Cl_2$ ($\mathbf{I_{Fe}}$),[15] and $TBA_7H_{11}[Co(A\text{-}\alpha\text{-}SiW_9O_{34})_2]\cdot 2H_2O\cdot C_2H_4Cl_2$ ($\mathbf{I_{Co}}$)[15] were synthesized according to the reported procedure. $Fe(acac)_3$ and $Mn(acac)_3$ were obtained from TCI. $Co(acac)_2\cdot 2H_2O$, $Ni(acac)_2\cdot 2H_2O$, and $Cu(OAc)_2\cdot 2H_2O$ were obtained from Kanto Chemical. $Ga(acac)_3$ was obtained from Aldrich. Solvents were obtained from Wako Pure Chemical Industries and Kanto Chemical and used as received.

Instruments

IR spectra were measured on JASCO FT/IR-4100 using KBr disks. Cold-spray ionization (CSI) mass spectra were recorded on JEOL JMS-T100CS. Thermogravimetric and differential thermal analyses (TG-DTA) were performed on Rigaku Thermo plus TG 8120. ICP-AES analyses were performed on Shimadzu ICPS-8100. Elemental analyses for C, H, N were performed on Yanaco MT-6 at the Elemental Analysis Center of School of Science, the University of Tokyo.

X-ray crystallography

Diffraction measurements were made on a Rigaku MicroMax-007 Saturn 724 CCD detector with graphite monochromated Mo K□ radiation (λ = 0.71069 Å) at 123 or 113 K. The data were collected and processed using CrystalClear[19] and HKL2000.[20] Neutral scattering factors were obtained from the standard source. In the reduction of data, Lorentz and polarization corrections were made. The structural analyses were performed using CrystalStructure,[21] WinGX,[22] and Yadokari-XG.[23] All structures were solved by SHELXS and refined by full-matrix least-squares methods using SHELXL.[24] The metal atoms (Si, W, Mn, Fe, Co, Ni, Ga) and oxygen atoms in the POM frameworks were refined anisotropically. CCDC-1049411 (**Mn5**), CCDC-1049412 ($\mathbf{II_{FeMn4}}$), CCDC-1049413 ($\mathbf{II_{CoMn4}}$), CCDC-1049414 ($\mathbf{II_{NiMn4}}$), CCDC-1049415 ($\mathbf{II_{CuMn4}}$), CCDC-1049416 ($\mathbf{II_{GaMn4}}$), CCDC-1049417 ($\mathbf{I_{Ni}}$), CCDC-1049418 ($\mathbf{I_{Cu}}$), and CCDC-1049419 ($\mathbf{I_{Ga}}$) contain the supplementary crystallographic data for this paper. The data can be obtained free of charge via www.ccdc.cam.ac.uk/conts/retrieving.html (or from the Cambridge Crystallographic Data Centre, 12, Union Road, Cambridge CB2 1EZ, UK; Fax: (+44) 1223-336-033; or deposit@ccdc.cam.ac.uk).

Magnetic measurements

Magnetic susceptibility data of the polycrystalline samples were measured on Quantum Design MPMS-XL7. Dc magnetic susceptibility measurements were carried out under the applied field of 0.1 T in the temperature range of 1.9–300 K. Variable-field magnetization measurements were carried out in the temperature range of 1.9–10 K. Ac magnetic susceptibility measurements were carried out under the 3.96 Oe ac oscillating field. Magnetization measurements at 0.5 K were carried out using IQUANTUM iHelium3. Diamagnetic corrections were applied by using Pascal constants and diamagnetisms of the sample holder and **SiW9**.

Acknowledgements

This work was supported in part by a Grant-in-Aid for Scientific Research from the Ministry of Education, Culture, Science, Sports, and Technology of Japan (MEXT).

Notes and references

1 (*a*) M. T. Pope, *Heteropoly and Isopoly Oxometalates*, Springer, Berlin, 1983; (*b*) N. Mizuno and M. Misono, *Chem. Rev.*, 1998, **98**, 199–218; (*c*) R. Neumann, *Prog. Inorg. Chem.*, 1998, **47**, 317–370; (*d*) C. L. Hill, in *Comprehensive Coordination Chemistry II, Vol. 4* (Eds.: J. A. McCleverty, T. J. Meyer), Elsevier Pergamon, Amsterdam, 2004, pp. 679–759; (*e*) D.-L. Long, R. Tsunashima and L. Cronin, *Angew. Chem. Int. Ed.*, 2010, **49**, 1736–1758.

2 (*a*) P. Putaj and F. Lefebvre, *Coord. Chem. Rev.*, 2011, **255**, 1642–1685; (*b*) P. Mialane, A. Dolbecq, E. Rivière, J. Marrot and F. Sécheresse, *Angew. Chem. Int. Ed.*, 2004, **43**, 2274–2277; (*c*) B. S. Bassil, M. Ibrahim, R. Al-Oweini, M. Asano, Z. Wang, J. van Tol, N. S. Dalal, K.-Y. Choi, R. N. Biboum, B. Keita, L. Nadjo and U. Kortz, *Angew. Chem. Int. Ed.*, 2011, **50**, 5961–5964; (*d*) Y. Hou, L. Xu, M. J. Cichon, S. Lense, K. I. Hardcastle and C. L. Hill, *Inorg. Chem.*, 2010, **49**, 4125–4132; (*e*) X.-B. Han, Z.-M. Zhang, T. Zhang, Y.-G. Li, W. Lin, W. You, Z.-M. Su and E.-B. Wang, *J. Am. Chem. Soc.*, 2014, **136**, 5359–5366; (*f*) C. Zhan, J. M. Cameron, J. Gao, J. W. Purcell, D.-L. Long and L. Cronin, *Angew. Chem. Int. Ed.*, 2014, **53**, 10362–10366.

3 (*a*) V. K. Yachandra, K. Sauer and M. P. Klein, *Chem. Rev.*, 1996, **96**, 2927–2950; (*b*) Y. Umena, K. Kawakami, J.-R. Shen and N. Kamiya, *Nature*, 2011, **473**, 55–60.

4 (*a*) R. Sessoli, D. Gatteschi, A. Caneschi and M. A. Novak, *Nature*, 1993, **365**, 141–143; (*b*) S. M. J. Aubin, N. R. Dilley, L. Pardi, J. Krzystek, M. W. Wemple, L. Brunel, M. B. Maple, G. Christou and D. N. Hendrickson, *J. Am. Chem. Soc.*, 1998, **120**, 4991–5004; (*c*) H. Miyasaka, R. Clérac, W. Wernsdorfer, L. Lecren, C. Bonhomme, K. Sugiura and M. Yamashita, *Angew. Chem. Int. Ed.*, 2004, **43**, 2801–2805; (*d*) C. J. Milios, A. Vinslava, W. Wernsdorfer, S. A. Moggach, S. Parsons, S. P. Perlepes, G. Christou and E. K. Brechin, *J. Am. Chem. Soc.*, 2007, **129**, 2754–2755; (*e*) H. Oshio, M. Nihei, S. Koizumi, T. Shiga, H. Nojiri, M. Nakano, N. Shirakawa and M. Akatsu, *J. Am. Chem. Soc.*, 2005, **127**, 4568–4569; (*f*) D. Li, S. Parkin, G. Wang, G. T. Yee, R. Clérac, W. Wernsdorfer and S. M. Holmes, *J. Am. Chem. Soc.*, 2006, **128**, 4214–4215; (*g*) A. Das, K. Gieb, Y. Krupskaya, S. Demeshko, S. Dechert, R. Klingeler, V. Kataev, B. Büchner, P. Müller and F. Meyer, *J. Am. Chem. Soc.*, 2011, **133**, 3433–3443.

5 (*a*) J. S. Kanady, E. Y. Tsui, M. W. Day and T. Agapie, *Science*, 2011, **333**, 733–736; (*b*) E. Y. Tsui, R. Tran, J. Yano and T. Agapie, *Nat. Chem.*, 2013, **5**, 293–299; (*c*) H. Yoon, Y.-M. Lee, X. Wu, K.-B. Cho, R. Sarangi, W. Nam and S. Fukuzumi, *J. Am. Chem. Soc.*, 2013, **135**, 9186–9194.

6 (*a*) Y. Kikukawa, K. Yamaguchi and N. Mizuno, *Angew. Chem. Int. Ed.*, 2010, **49**, 6096–6100; (*b*) K. Suzuki, Y. Kikukawa, S. Uchida, H. Tokoro, K. Imoto, S. Ohkoshi and N. Mizuno, *Angew. Chem. Int. Ed.*, 2012, **51**, 1597–1601; (*c*) T. Hirano, K. Uehara, K. Kamata and N. Mizuno, *J. Am. Chem. Soc.*, 2012, **134**, 6425–6433; (*d*) Y. Kikukawa, K. Suzuki, M. Sugawa, T. Hirano, K. Kamata, K. Yamaguchi and N. Mizuno, *Angew. Chem. Int. Ed.*, 2012, **51**, 3686–3690; (*e*) K. Suzuki, R. Sato and N. Mizuno, *Chem. Sci.*, 2013, **4**, 596–600; (*f*) R. Sato, K. Suzuki, M. Sugawa and N. Mizuno, *Chem. Eur. J.*, 2013, **19**, 12982–12990; (*g*) K. Suzuki, F. Tang, Y. Kikukawa, K. Yamaguchi and N. Mizuno, *Angew. Chem. Int. Ed.*, 2014, **53**, 5356–5360.

7 There have been several reports on the synthesis of multinuclear manganese-containing POMs in aqueous media: (*a*) R. Al-Oweini, B. S. Bassil, J. Friedl, V. Kottisch, M. Ibrahim, M. Asano, B. Keita, G. Novitchi, Y. Lan, A. Powell, U. Stimming and U. Kortz, *Inorg. Chem.*, 2014, **53**, 5663–5673; (*b*) C. J. Gómez-García, J. J. Borras-Almenar, E. Coronado and L. Ouahab, *Inorg. Chem.*, 1994, **33**, 4016–4022; (*c*) C. J. Gómez-García, E. Coronado, P. Gómez-Romero, N. Casañ-Pastor, 1993, **32**, 3378–3381.

8 T. Minato, K. Suzuki, K. Kamata and N. Mizuno, *Chem. Eur. J.*, 2014, **20**, 5946–5952.

9 The χT value at 1.9 K for **Mn5** was 3.66 cm^3 K mol^{-1} (Fig. 2). In addition, the fitting of the magnetization data of **Mn5** by the Hamiltonian given in eqn (1) afforded the parameters of $S = 2$, $D = -2.20$ cm^{-1}, $|E| = 1.0\times10^{-4}$ cm^{-1}, and $g = 2.01$.

10 The magnetization relaxation time τ was evaluated from the frequency dependence of χ'' signals at each temperature (Fig. S2, ESI†).

11 The analyses were carried out by using PHI program: N. F. Chilton, R. P. Anderson, L. D. Turner, A. Soncini and K. S. Murray, *J. Comput. Chem.*, 2013, **34**, 1164–1175.

12 (*a*) W. Chen, Y. Li, Y. Wang, E. Wang and Z. Zhang, *Dalton Trans.*, 2008, 865–867; (*b*) J. Wang, W. Wang and J. Niu, *J. Mol. Struct.*, 2008, **873**, 29–34; (*c*) A. Merca, A. Müller, J. van Slageren, M. Läge and B. Krebs, *J. Clust. Sci.*, 2007, **18**, 711–719.

13 (*a*) Y.-W. Li, Y.-G. Li, Y.-H. Wang, X.-J. Feng, Y. Lu and E.-B. Wang, *Inorg. Chem.*, 2009, **48**, 6452–6458; (*b*) Z.-M. Zhang, Y.-G. Li, S. Yao and E.-B. Wang, *Dalton Trans.*, 2011, **40**, 6475–6479.

14 (*a*) T. M. Anderson, K. I. Hardcastle, N. Okun and C. L. Hill, *Inorg, Chem.*, 2001, **40**, 6418–6425; (*b*) T. M. Anderson, X. Zhang, K. I. Hardcastle and C. L. Hill, *Inorg, Chem.*, 2002, **41**, 2477–2488; (*c*) I. M. Mbomekalle, B. Keita, L. Nadjo, W. A. Neiwert, L. Zhang, K. I. Hardcastle, C. L. Hill and T. M. Anderson, *Eur. J. Inorg. Chem.*, 2003, 3924–3928; (*d*) L. Ruhlmann, C. Costa-Coquelard, J. Canny and R. Thouvenot, *Eur. J. Inorg. Chem.*, 2007, 1493–1500; (*e*) C. M. Tourné, G. F. Tourné and F. Zonnevijlle, *J. Chem. Soc., Dalton Trans.*, 1991, 143–155; (*f*) S. Reinoso and J. R. G.-Mascarós, *Inorg. Chem.*, 2010, **49**, 377–379; (*g*) R. Cao, K. P. O'Halloran, D. A. Hillesheim, S. Lense, K. I. Hardcastle and C. L. Hill, *CrystEngComm*, 2011, **13**, 738–740; (*h*) S. Reinoso, J. R. G.-Mascarós and L. Lezama, *Inorg. Chem.*, 2011, **50**, 9587–9593.

15 R. Sato, K. Suzuki, T. Minato, M. Shinoe, K, Yamaguchi and N. Mizuno, *Chem. Commun.*, 2015, **51**, 4081–4084.

16 Compounds $\mathbf{I_{Ni}}$, $\mathbf{I_{Cu}}$, and $\mathbf{I_{Ga}}$ were synthesized by the same procedure as that for $\mathbf{I_{Fe}}$ using $Ni(acac)_2$, $Cu(OAc)_2$, and $Ga(acac)_3$ as the metal sources (Figs. S20–S22, Table S9, ESI†).

17 (*a*) C. Ritchie, A. Ferguson, H. Nojiri, H. N. Miras, Y.-F. Song, D.-L. Long, E. Burkholder, M. Murrie, P. Kögerler, E. K. Brechin and L. Cronin, *Angew. Chem. Int. Ed.*, 2008, **47**, 5609–5612; (*b*) J.-D. Compain, P. Mialane, A. Dolbecq, I. M. Mbomekallé, J. Marrot, F. Sécheresse, E. Rivière, G. Rogez and W. Wernsdorfer, *Angew. Chem. Int. Ed.*, 2009, **48**, 3077–3081; (*c*) X. Fang, M. Speldrich, H. Schilder, R. Cao, K. P. O'Halloran, C. L. Hill and P. Kögerler, *Chem. Commun.*, 2010, **46**, 2760–2762; (*d*) M. Ibrahim, Y. Lan, B. S. Bassil, Y. Xiang, A. Suchopar, A. K. Powell and U. Kortz, *Angew. Chem. Int. Ed.*, 2011, **50**, 4708–4711; (*e*) Y. Sawada, W. Kosaka, Y. Hayashi and H. Miyasaka, *Inorg. Chem.*, 2012, **51**, 4824–4832; (*f*) H. E. Moll, A. Dolbecq, J. Marrot, G. Rousseau, M. Haouas, F. Taulelle, G. Rogez, W. Wernsdorfer, B. Keita and P. Mialane, *Chem. Eur. J.*, 2012, **18**, 3845–3849; (*g*) Z.-M. Zhang, S. Yao, Y.-G. Li, H.-H. Wu, Y.-H. Wang, M. Rouzières, R. Clérac, Z.-M. Su and E.-B. Wang, *Chem. Commun.*, 2013, **49**, 2515–2517.

18 D. Gatteschi, R. Sessoli and J. Villain, *Molecular Nanomagnets*, Oxford University Press, Oxford, 2006.

19 (*a*) *CrystalClear* 1.3.6, Rigaku and Rigaku/MSC, The Woodlands, TX; (*b*) J. W. Pflugrath, *Acta Crystallogr.*, 1999, **D55**, 1718–1725.

20 Z. Otwinowski and W. Minor, Processing of X-ray Diffraction Data Collected in Oscillation Mode. in *Methods in Enzymology*, C. W. Carter, Jr., R. M. Sweet, Eds., Macromolecular Crystallography, Part A, Academic press, New York, 1997, Vol. 276, pp. 307–326.

21 *CrystalStructure* 3.8, Rigaku and Rigaku/MSC, The Woodlands, TX.

22 L. J. Farrugia, *J. Appl. Crystallogr.*, 1999, **32**, 837–838.

23 Yadokari-XG, Software for Crystal Structure Analyses, K. Wakita, 2001; Release of Software (Yadokari-XG 2009) for Crystal Structure Analyses, C. Kabuto, S. Akine, T. Nemoto and E. Kwon, *J. Cryst. Soc. Jpn.*, 2009, **51**, 218–224.
24 G. M. Sheldrick, SHELX97, *Programs for Crystal Structure Analysis*, Release 97-2, University of Göttingen, Göttingen, Germany, 1997.

Graphical Abstract

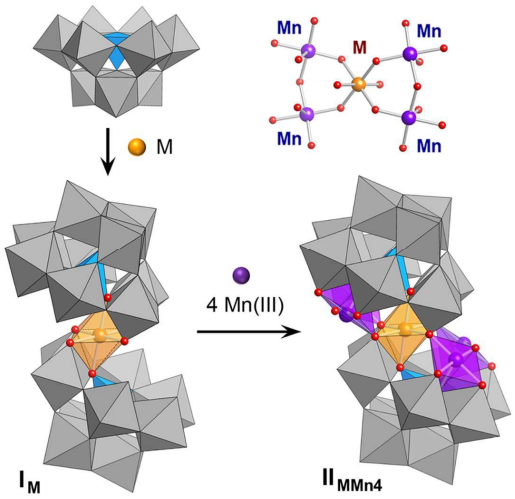

Hetero-pentanuclear clusters {MMn_4} were successfully synthesized in polyoxometalates (POMs) by sequential introduction of metal cations into the trivacant lacunary POMs, and the clusters showed the large magnetic anisotropy and the SMM behavior.